



Open Archive Toulouse Archive Ouverte (OATAO)

OATAO is an open access repository that collects the work of Toulouse researchers and makes it freely available over the web where possible.

This is an author-deposited version published in: <http://oatao.univ-toulouse.fr/>
Eprints ID: 6304

To link to this article: DOI:10.1016/j.proeng.2011.04.258
<http://dx.doi.org/10.1016/j.proeng.2011.04.258>

To cite this version:

Msolli, Sabeur and Dalverny, Olivier and Alexis, Joël and Karama, Moussa
Implicit integration scheme for porous viscoplastic potential-based constitutive equations. (2011) *Procedia Engineering*, vol. 10 . pp. 1544-1549. ISSN 1877-7058

Any correspondence concerning this service should be sent to the repository administrator:
staff-oatao@inp-toulouse.fr

ICM11

Implicit integration scheme for porous viscoplastic potential-based constitutive equations

S. Msolli^{a,*}, O. Dalverny^a, J. Alexis^a, M. Karama^a

^a *Université de Toulouse ; INP/ENIT ; LGP ; 47, avenue d'Azereix ; F-65016 Tarbes, France*

Abstract

This paper deals with a viscoplastic potential-based model allowing thermomechanical damage behavior modeling of porous materials. The model describes rate dependent effects, hardening, creep as well as defects coalescence and propagation. Kinematic and isotropic hardening effects are taken into account by a set of internal state variables. The integration and implementation of the model into the FE code using a fully implicit integration scheme is exposed. Finally, it's used to predict mechanical behaviour degradation of solder layers used in power electronic packaging. Stress-strain behaviour and the evolution of volumic fraction of voids for the material under cyclic loading are presented.

Keywords : Viscoplastic, Porous, Potential, Integration scheme, FEM

1. Introduction

Solder joints are basic parts in power electronic modules which are subjected to severe thermomechanical cyclic loading, involving fatigue and creep at high temperatures [1,2]. Many factors could have influence on the solder behaviour. Among these factors, we note the metallurgical aspect and the initial state of the solder material, the amount of porosity in the layer, the temperature history during the manufacturing stages. All these factors induced a set of defects of solder matrix, and as resulting effects, they modify their thermomechanical behaviour leading to a fall in solder lifetime and so of the whole packaging assembly. Volumic fraction of porosity may be considerable within the total volume of the solder layer and thus leads to weaken the whole thermomechanical behaviour of the junction [3]. The

* Corresponding author. Tel.: +33 5 62 44 27 16; fax: +33 5 62 44 27 08.
E-mail address: smsolli@enit.fr

fact that lifetime is influenced by defects coming before and during service, proves the need of pertinent theoretical models which are able to reproduce entire material behaviour during thermal-mechanical loading cycles and to accurately predict material degradation. The models have to take into account hardening variables and porous damage for viscoplastic materials which still a challenging task.

Nomenclature

C_{ijkl}	Fourth order elasticity tensor
\tilde{C}_{ijkl}	Fourth order damaged elasticity tensor
I_{ijkl}	Fourth order unit tensor
δ_{ij}	Second order unit tensor
G	Shear modulus (MPa)
E	Young modulus (MPa)
κ, μ	Lamé elastic modulus (MPa)
ν	Poisson ratio
α	Coefficient of Thermal Expansion (ppm/K)
$n = 1/m$	Sensitivity parameter to inelastic strain rate
Q	Activation energy (J/mol)
R_G	Gaz constant (8.314 J/mol.K)
R	Dragstress variable (MPa)
T	Absolute temperature (K)
T_f	Melting temperature (K)
k	Boltzmann constant
R^0	initial yield stress (MPa)
f_0	Initial volumic fraction of voids
f_n	Density of void nuclei
ϵ_n	Mean value of the Gauss distribution
s_n	Width of the Gauss distribution
D	isotropic resistance to plastic deformation (MPa)
$J = \sqrt{\frac{3}{2} o'_{ij} : o'_{ij}}$	Second invariant of the o deviator tensor
σ_{ij}, s_{ij}	Stress and deviator stress tensors (MPa)
$\alpha_{ij}^{(k)}$	Backstress tensor (MPa) $k = 1, 2$
ϵ_{ij}^e	Elastic tensor
ϵ_{ij}^{in}	Inelastic strain tensor
A_0	Pre-exponential material parameter
Δp	Effective inelastic strain increment
$D_f < 1$	Coefficient relating the surfacic to the volumic fraction of voids
B	Temperature-independent material parameters
$\bar{\chi}$	Isotropic saturation limit (MPa)
μ'	Isotropic hardening rate
C_k	Hardening modulus
b_k	Hardening rate controlling parameter

2. Formulation of the viscoplastic constitutive equations

We introduce an internal state variable based unified viscoplastic model combined with a porous damage as first step for the viscoplastic-damage predictions. The damage model is based on Hagni and Anand framework [4], which considers a Duva and Hutchinson approaches [5], for the evolution of the volumic fraction of voids. As for the existing unified models, the constitutive equations are composed of a flow law for the inelastic deformation and a set of evolution equations for the state variables. From the thermodynamic viewpoint, the inelastic flow is derived from the free Helmholtz energy. This free energy depends on the volumic fractions of voids f and the internal state variables. Once the free energy expressed, then the flow law and the state variables can be directly derived from it. In our case, the kinematic and isotropic hardening rules are expressed respectively as:

$$\dot{\alpha}_{ij}^{(k)} = (1-f) \left(C_k b_k \dot{\varepsilon}_{ij}^{in} - C_k \alpha_{ij}^{(k)} \dot{p} + \left[\omega \frac{\alpha_{ij}^{(k)}}{b_k} \frac{\chi}{\mu \bar{\chi}} \frac{\partial(\mu \bar{\chi})}{\partial T} + \frac{\alpha_{ij}^{(k)}}{C_k} \frac{\partial C_k}{\partial T} + \frac{\alpha_{ij}^{(k)}}{b_k} \frac{\partial b^0}{\partial T} \right] \dot{T} - C_k b_k \Omega_i^\alpha \theta \alpha_i \right) \quad (1)$$

$$\dot{\chi} = (1-f) \left(\mu(\bar{\chi} - \chi) \dot{p} + \frac{\chi}{\mu \bar{\chi}} \frac{\partial(\mu \bar{\chi})}{\partial T} \dot{T} - \mu \bar{\chi} \Omega^\alpha \theta \right) \quad (2)$$

Where $\dot{p} = \sqrt{\frac{2}{3} \dot{\varepsilon}_{ij}^{in} : \dot{\varepsilon}_{ij}^{in}}$ is the effective inelastic strain rate. Thus, the total backstress is expressed as the sum of the $\alpha_{ij}^{(k)}$ such as $\alpha_{ij} = \sum_k \alpha_{ij}^{(k)}$. Note that the kinematic hardening formulation could represent

hardening, dynamic recovery and static thermal recovery effects. Description of thermal variation effects is also improved by introducing the energy activation term in the static thermal recovery term.

Let's remember that for virgin materials, the inelastic flow rate is derived from a viscoplastic potential Φ , which could be expressed in our case as follows:

$$\Phi = \frac{D}{B \left(\frac{1}{m} + 1 \right)} A \Theta \exp \left[B \zeta^{\frac{1}{m} + 1} \right] \quad (3)$$

Where ζ is expressed as:

$$\zeta = \left\langle \frac{J \left(\sigma_{ij} - \sum_k \alpha_{ij}^{(k)} \right) - R - R^0}{D} \right\rangle \quad (4)$$

and, Θ is a thermal diffusivity parameter expressed as an Arrhenius function.

$$\Theta = \begin{cases} \exp \left(-\frac{Q}{kT} \right) & \text{for } T \geq \frac{T_m}{2} \\ \exp \left(-\frac{2Q}{kT_m} \left\{ \ln \left(\frac{T_m}{2T} \right) + 1 \right\} \right) & \text{for } T \leq \frac{T_m}{2} \end{cases} \quad (5)$$

$\langle g \rangle$ is defined as g if $g \geq 0$ else $g = 0$.

By introducing the volumic fraction of voids f , the viscoplastic potential for porous materials is calculated using Duva and Hutchinson approaches based on the expression:

$$\Phi_p = F \times \Phi \quad (6)$$

F is given by Hagni and Anand as function of the effective stress triaxiality X and takes the form:

$$F = 1 + \frac{f}{m} \left[C^{2/(1/m)+1} \left\{ \frac{3}{2} mX \right\}^2 + g \right]^{((1/m)+1)/2} \quad (7)$$

Where $X = \frac{\sigma_{mm} - \sum_k \alpha_{mm}^{(k)}}{J \left(\sigma_{ij} - \sum_k \alpha_{ij}^{(k)} \right)}$ and $C = \frac{1}{(1-f^m)^{1/m}}$. C is used here for voids interaction effects.

Usually, g is assumed to be constant and takes the value of 1.3 for a corresponding value of 0.161 for m . From Zavaliangos and Anand [6], an alternative form of $g(f,m)$ is applicable for a wide range of m and is written as:

$$g(f, m) = \left[\frac{m}{f} (F_0 - 1) \right]^{-2/(1+1/m)} \quad (8)$$

Where

$$F_0 = \left(\frac{1 + 3,34f + 0,25f^2}{1 - f^2} \right)^{1/(2m)} \quad (9)$$

The evolution of the volumic fraction of voids is governed by the next equation taking into account void nucleation and neglecting elastic compressibility.

$$\dot{f} = \dot{f}_G + \dot{f}_N = (1-f) \dot{\varepsilon}_{mm}^{in} + A_N \dot{p} \quad (10)$$

where $A_N = \frac{f_N}{s_N \sqrt{2\pi}} \exp \left(-\frac{1}{2} \left(\frac{p - \varepsilon_N}{s_N} \right)^2 \right)$ means that nucleation is governed by a Gauss distribution.

Finally, the normality rules permit to determine the inelastic flow law by deriving the porous viscoplastic potential expression in order to have,

$$\dot{\varepsilon}_{ij}^{in} = \frac{\partial \Phi_p}{\partial \sigma_{ij}} \quad (11)$$

The built model in its actual form makes it possible to take into account kinematic and isotropic hardening, time-dependent and time-independent effects, and degradation due to the volumic fraction of voids.

3. Development of the integration algorithm

The model is composed of a set of differential constitutive equations. Weber and Anand developed an integration scheme for isothermal deformations of fully dense materials [7]. Zavaliangos and Anand presented an extension of this scheme for porous materials based on Zavaliangos framework [8]. The aim of this fully implicit, fully coupled integration scheme is to find the solution of the following equation.

$$h(\Delta \varepsilon_{ij}^{in}) = \Delta \varepsilon_{ij}^{in} - \frac{\partial \Phi}{\partial \sigma_{ij}} \Delta t \quad (12)$$

If we assume that $(\Delta \varepsilon_{ij}^{in})^{n+1}$ is the solution at iteration $n+1$, then we can write:

$$h\left((\Delta \varepsilon_{ij}^{in})^{n+1}\right) = h\left((\Delta \varepsilon_{ij}^{in})^n\right) + \frac{\partial h}{\partial \Delta \varepsilon_{kl}^{in}} : \left((\Delta \varepsilon_{ij}^{in})^{n+1} - (\Delta \varepsilon_{ij}^{in})^n \right) = 0 \quad (13)$$

That allows determining the solution increment by transforming equation (13) into,

$$(\Delta \varepsilon_{ij}^{in})^{n+1} = - \left[\frac{\partial h}{\partial \Delta \varepsilon_{kl}^{in}} \right]^{-1} : h\left((\Delta \varepsilon_{ij}^{in})^n\right) + (\Delta \varepsilon_{ij}^{in})^n \quad (14)$$

The value of $(\Delta \varepsilon_{ij}^{in})^{n+1}$ is then calculated by a Newton-Raphson iteration scheme.

As a result, if the relative error $\left\| \frac{(\Delta \varepsilon_{ij}^{in})^{n+1} - (\Delta \varepsilon_{ij}^{in})^n}{(\Delta \varepsilon_{ij}^{in})^{n+1}} \right\| \leq \varepsilon^{tol}$, the solution is retained, else the calculation is

repeated for the next iteration step $n + 1$. The integration algorithm is resumed in the following steps below:

- ① - Assume an inelastic strain increment tensor
- ② - Compute the volumic fraction of voids using equation (10)
- ③ - Compute the variables of Haghi and Anand damage model using (7), (8), and (9)
- ④ - Compute the trial stress tensor using Hooke's law.
- ⑤ - Compute the effective stress triaxiality X
- ⑥ - Compute the internal state variables in the equations (1) and (2)
- ⑦ - Compute residual function $\|h_{ij}\|$
 - a - **If** the residual function is less than the fixed tolerance **then** retain computed variables and stress as solution and go to next increment.
 - b - **Else** update inelastic strain increment using (14) and go to step ②.

4. Numerical results

The exposed algorithm was implemented in the Abaqus® FE code. Pure mechanical tests on Sn96Ag3Cu1 solder were used to prove the capability of the model. In this way, we first simulate uniaxial tensile and relaxation tests with many strain rate conditions. The simulations results shown in figure 1 and 2, proved the accuracy of the algorithm.

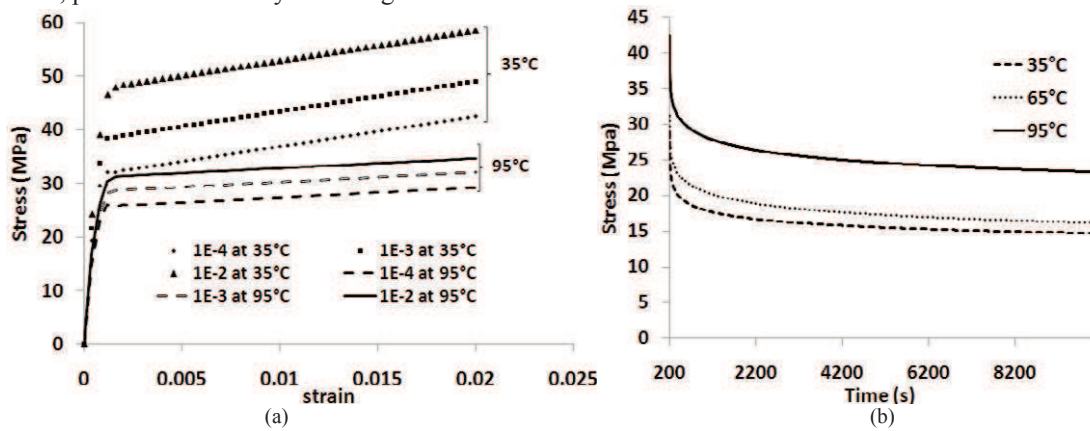


Fig. 1. Uniaxial simulated tests at various temperatures, (a) tensile curves at different strain rates, (b) relaxation curves

Figure 1(a) shows the ability of the model to reproduce recovery effects. In the case of SnAgCu, kinematic hardening is dominant, and the saturation of stress is observable especially at high temperature. We denote a reduction of the final stress from 60 MPa at 35°C to nearly 30 MPa at 95°C. On figure 1(b) relaxation tests at various temperatures demonstrate the effect of the thermal or static recovery on the stress response. In a second way, we've simulated cyclic tests to illustrate the damage behaviour coupled with the viscoplastic law. In the ten first cycles of the tensile loading, the mean volumic fraction of voids is constant so it means that there is no nucleation of voids but only regular voids growth due to "open-close" cycles (Figure 2(a) stage A). This fact is improved also by taken into account voids shrinkage.

Afterwards, nucleation effects are more apparent (Figure 2(a) stage B), and the mean value of the voids fraction increases continuously due to the increase of inelastic deformation until a value of 5.5×10^{-2} . The density of void nuclei f_n is in fact activated by equivalent plastic strain \dot{p} in the matrix. Starting from this value, the void fraction increases quite slowly which indicates a nearly saturated state in the material. At last, figure 2 (b) show volumic fraction of voids distribution around a hole drilled in a plate submitted to the uniaxial cyclic loading. The two stages, A and B, are illustrated.

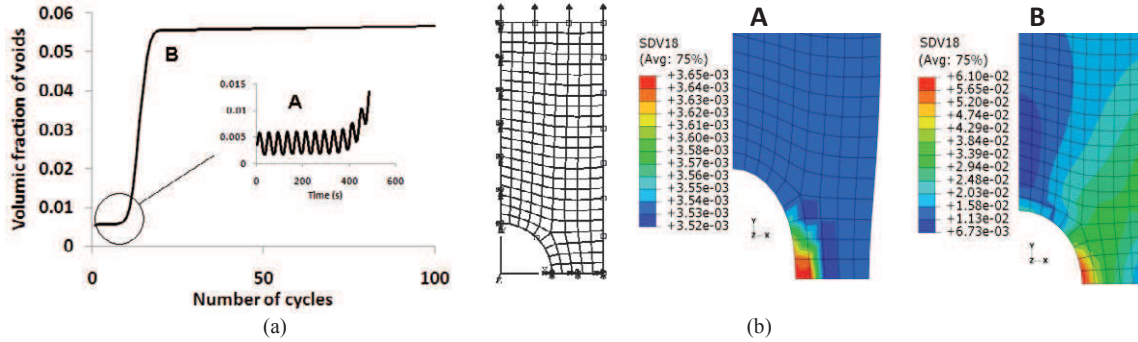


Fig. 2. Damage behavior of the model, (a) evolution of the volumic fraction of voids during cycling test, (b) volumic fraction of voids distribution around a hole at two stages (A and B) of the cycling test

5. Conclusion

Porous viscoplasticity in SnAgCu solder is studied within a porous viscoplastic potential-based model. The model assumes an initial uniform distribution of voids in the whole volume and follows the phenomenological concept of internal state variables is able to describe hardening, creep and static thermal recovery among others. The implicit integration scheme proves to be stable and successfully implemented into finite element code Abaqus®. Effect of nucleation is observed clearly after the first few cycles and increases under a nearly saturated level of about 6×10^{-2} .

References

- [1] Tien JK, Hendrix BC and Attarwala AI. Creep-fatigue interactions in solders. *IEEE transactions on Components, Hybrids, And Manufacturing Technology*. 1989;**12**:502-505.
- [2] Micol A, Zéanah A, Lhommeau T, Azzopardi S, Woigard E, Dalverny O, and Karama M. An investigation into the reliability of power modules considering base plate solders thermal fatigue in aeronautical applications. *Microelectronics Reliability* 2009;**49**:1370-1374.
- [3] Dudek MA, Hunter L, Kranz S, Williams JJ, Lau SH and Chawla N. Three-dimensional (3D) visualization of reflow porosity and modeling of deformation in Pb-free solder joints. *Materials Characterization* 2010;**61**:433-439.
- [4] Haghi M and Anand L. A constitutive model for isotropic, porous, elastic-viscoplastic metals. *Mechanics of Materials* 1992;**13**:37-53.
- [5] Duva JM and Hutchinson JW. Constitutive potentials for dilutely voided nonlinear materials. *Mechanics of Materials* 1984;**3**:41-54.
- [6] Zavaliangos A and Anand L. Thermo-elasto-viscoplasticity of isotropic porous materials. *Journal of the Mechanics and Physics of Solids* 1993;**41**: 1087-1118.
- [7] Weber G and Anand L. Finite deformation constitutive equations and a time integration procedure for isotropic, hyperelastic-viscoplastic solids. *Computer Methods in Applied Mechanics and Engineering* 1990;**79**: 173-202.
- [8] Zavaliangos A and Anand L. Towards a Capability for Predicting the Formation of Defects During Bulk Deformation Processing. *CIRP Annals - Manufacturing Technology* 1991;**40**: 267-271.